International Journal of Pharmaceutics 517 (2017) 226–233

Contents lists available at ScienceDirect

International Journal of Pharmaceutics

journal homepage: www.elsevier.com/locate/ijpharm

NaCl strongly modifies the physicochemical properties of aluminum hydroxide vaccine adjuvants

Jean-François Art, Aurélien vander Straeten, Christine C. Dupont-Gillain*

Université catholique de Louvain, Institute of Condensed Matter and Nanosciences, Bio- and Soft Matter Division, Place Louis Pasteur 1/L4.01.10, 1348 Louvain-la-Neuve, Belgium

ARTICLE INFO

Article history:
Received 28 October 2016
Received in revised form 5 December 2016
Accepted 8 December 2016
Available online 9 December 2016

Keywords:
Vaccine formulation
Aluminum hydroxide adjuvant
Ionic strength
Sodium chloride
XPS
AFM
Specific surface area

ABSTRACT

The immunostimulation capacity of most vaccines is enhanced through antigen adsorption on aluminum hydroxide (AH) adjuvants. Varying the adsorption conditions, i.e. pH and ionic strength (I), changes the antigen adsorbed amount and therefore the ability of the vaccine to stimulate the immune system. Vaccine formulations are thus resulting from an empirical screening of the adsorption conditions. This work aims at studying the physicochemical effects of adjusting the ionic strength of commercial AH adjuvant particles suspensions with sodium chloride (NaCl). X-ray photoelectron spectroscopy data show that AH particles surface chemical composition is neither altered by I adjustment with NaCl nor by deposition on gold surfaces. The latter result provides the opportunity to use AH-coated gold surfaces as a platform for advanced surface analysis of adjuvant particles, *e.g.* by atomic force microscopy (AFM). The morphology of adjuvant particles recovered from native and NaCl-treated AH suspensions, as studied by scanning electron microscopy and AFM, reveals that AH particles aggregation state is significantly altered by NaCl addition. This is further confirmed by nitrogen adsorption experiments: I adjustment to 150 mM with NaCl strongly promotes AH particles aggregation leading to a strong decrease of the developed specific surface area. This work thus evidences the effect of NaCl on AH adjuvant structure, which may lead to alteration of formulated vaccines and to misinterpretation of data related to antigen adsorption on adjuvant particles.

1. Introduction

Vaccination plays an important role in preventing many infectious diseases. Vaccines prepared from attenuated or killed pathogens are directly effective and elicit a sufficient immune response. Nowadays, vaccines produced from antigenic subunits of pathogens, such as proteins or polysaccharides, or from pathogens toxoids, such as tetanus or diphtheria toxoids (Singh et al., 2006), are better tolerated by the body but also less immunogenic. They therefore fail to trigger both sufficient immune response and memory effect (Eppstein et al., 1989; Mbow et al., 2010), especially in children (Sivakumar et al., 2011). In 1926, Glenny et al. observed that diphtheria toxoid precipitated in presence of potassium alum ($KAl(SO_4)_2$) gave a higher immune response than the soluble toxoid after injection to guinea pigs (HogenEsch, 2002). The first adjuvant effect was just discovered.

Since then, many types of vaccine adjuvants have been studied, from bacterial extracts to emulsions passing by specialty polymers (Eppstein et al., 1989; Mbow et al., 2010; Sivakumar et al., 2011). These adjuvants have been used in vaccines with the objective to elicit a sufficient immune response and to limit secondary effects (Aguilar and Rodríguez, 2007; O'Hagan et al., 2001). Nowadays, the more widespread adjuvants used in human vaccines are aluminum-based suspensions. Commercially-used aluminum-containing adjuvants in vaccine formulation are prepared by precipitation of aluminum salts in controlled alkaline conditions (Lindblad, 2004).

Precipitation performed in presence of phosphate ions results in an amorphous gel of a non-stoichiometric compound having an $Al(PO_4)_x(OH)_y$ formula and commonly known as aluminum phosphate (AP) adjuvant. AP adjuvant is composed of platelet particles with a diameter of 50 nm forming irregular aggregates of 1–20 μm. The production process as well as different physicochemical characteristics of AP adjuvants have been well described in the literature (Burrell et al., 2000a, 2000b). Commercial AP adjuvants are composed of particles suspended in a NaCl solution.

* Corresponding author.
E-mail addresses: jean-francois.art@uclouvain.be (J.-F. Art), aurelien.vanderstraeten@uclouvain.be (A. vander Straeten), christine.dupont@uclouvain.be (C.C. Dupont-Gillain).

http://dx.doi.org/10.1016/j.ijpharm.2016.12.019
0378-5173/

When the precipitation process is performed without added ions, an amorphous gel of aluminum hydroxide ($Al(OH)_3$) is obtained. Commercial aluminum hydroxide (AH) adjuvant is actually poorly crystalline boehmite. It is composed of a mixture of amorphous $Al(OH)_3$ and hydrated crystalline aluminum oxyhydroxide $AlOOH{\cdot}nH_2O$ (Hem and White, 1995; Shirodkar et al., 1990). This organized fraction is obtained by a hydrothermal treatment causing the dehydration of the primary $Al(OH)_3$ gel according to the following reaction:

$$Al(OH)_{3\ amorphous} \rightarrow AlOOH_{crystalline} + H_2O$$

Mineralogists have shown that AlOOH formation by dehydration of $Al(OH)_3$ is facilitated by high temperature and high sodium chloride concentration (3 M) (Tettenhorst and Hofmann, 1980; Yau et al., 2006). Adjuvant hydroxyl groups are coordinated with aluminum atoms. The surface charge of AH particles is pH-dependent, with a point of zero charge (PZC) of 11.4 (Rinella et al., 1998). Shirodkar et al. observed by transmission electron microscopy that AH adjuvants are composed of primary needle-like particles presenting the characteristic fibrous morphology of boehmite (Hem and White, 1995; Shirodkar et al., 1990), with average dimensions of $4.5 \times 2.2 \times 10\,nm^3$, and forming aggregates of 1–20 μm when dispersed in solution (Hem and HogenEsch, 2007). These aggregates are in dynamic equilibrium in suspension (aggregating and disaggregating continuously) and are known to be the functional units of adjuvants, i.e. the effective structure for antigen adsorption and immune system stimulation (Morefield et al., 2004). AH adjuvant specific surface area was determined by gravimetric/FTIR-based methods and X-ray diffraction (XRD) to be around $500\,m^2/g$ (Johnston et al., 2002). Stability studies of AH adjuvants over time or exposure to autoclaving showed that XRD spectra become sharper after treatment. It means that more order was developed in AH particles over time or after heat treatment as it enhances dehydration of amorphous $Al(OH)_3$ and formation of AlOOH. By acquiring more order, AH adjuvant showed a decrease in both specific surface area and adsorption capacity of antigens (Burrell et al., 1999, 2000c).

The World Health Organization (WHO) recommends for tetanus and diphtheria toxoids that 80% of antigen is adsorbed on adjuvant particles (Clausi et al., 2008). The antigenic subunits have indeed to be adsorbed on particles of an adjuvant suspension to produce an effective vaccine. It was shown that antigens adsorbed on aluminum-based adjuvants lead to a higher immune response compared to soluble antigens. Although mechanisms are still not completely understood, the higher immunostimulation of adsorbed antigens was explained by a prolonged retention time of aluminum-based adjuvants and adsorbed antigens at the injection site. This retention time, combined with a higher recruitment of immune system cells due to inflammatory response induced by adjuvants, is believed to have a positive effect on vaccine efficiency (Lindblad, 2004). Furthermore, Jones et al. showed that conformational changes of proteins upon adsorption on aluminum salts adjuvants lead to a higher immunogenicity of the vaccine. Antigen adsorption is thus considered as an important step of vaccine formulation (Jones et al., 2005).

To improve vaccine formulation, adsorption isotherms of model proteins were constructed experimentally to determine adjuvant adsorption capacity as well as involved mechanisms. Hem et al. showed that bovine serum albumin (BSA) and lysozyme respectively adsorbed on AH and AP suspensions at physiological pH (7.4). By rising the ionic strength (I) with NaCl, it was shown by Hem and coworkers that the adsorption capacity of BSA and lysozyme decreased on AH and AP, respectively. This was considered as a proof that electrostatic interactions were one of the major adsorption mechanisms of protein antigens on aluminum-based adjuvants (Al-Shakhshir et al., 1995; Hem and White, 1995). pH and I are thus tuned in the course of vaccine formulation to improve antigen adsorption.

The second principal driving force for antigen adsorption on adjuvant particles is believed to be a ligand exchange between antigen phosphate groups and adjuvant hydroxyl groups (Iyer et al., 2003; Morefield et al., 2005). This mechanism was deduced from the tunable adsorption of ovalbumin (OVA) on aluminum-based adjuvants. Highly phosphorylated OVA adsorbed more strongly and in higher amounts than dephosphorylated OVA on both AH and AP. As both adjuvants expose hydroxyl groups at the surface of particles, ligand exchange between hydroxyl and phosphate groups was proposed as adsorption mechanism. It was shown that the interaction force between adjuvant and antigen adsorbed by ligand exchange is stronger than by electrostatic interactions.

Adsorption of model antigens was often studied at pH 7.4 to be close to the physiological conditions of vaccines for parenteral administration. Regarding the latter administration way, the vaccine also needs to be as close as possible to the isotonicity, which is around 0.15 M in NaCl.

NaCl is thus frequently used in vaccine formulation (i) to optimize antigen adsorption and (ii) to adjust the vaccine I before injection. It was however shown that high NaCl concentration (3 M) during AH adjuvant production facilitates crystalline aluminum oxyhydroxide formation (Yau et al., 2006). As the formation of crystalline areas of AH adjuvant modifies its structure, vaccine efficiency could be modified after I adjustment. The potential effects on AH adjuvant structure of moderate NaCl concentration used to improve antigen adsorption or to adjust vaccine ionic strength have not been addressed yet.

This work aims at using advanced surface characterization techniques, i.e. atomic force microscopy and X-ray photoelectron spectroscopy, to characterize the effect of adding NaCl to commercial aluminum hydroxide adjuvant suspensions thereby mimicking the influence of body isotonicity. Adjuvant suspensions were used as such or after exposure to 150 mM NaCl and analyzed as freeze-dried powders or after deposition on a gold substrate depending on the further applied characterization method. Nitrogen adsorption, followed by computation of surface specific area, and scanning electron microscopy were also used to characterize the samples. Physicochemical properties such as surface chemical composition, particle morphology or developed specific surface area could indeed be modified upon exposure to NaCl during vaccine production steps. AH structure modification may finally alter vaccine efficiency.

2. Materials and methods

2.1. Materials

Two commercial aluminum hydroxide adjuvants were chosen for this work. ALHYDROGEL® “85” 2%–Ph. Eur. (AH1) was kindly provided by BRENNTAG (Brenntag Biosector, Denmark). REHYDRAGEL® LV (AH2) was purchased from General Chemical (NJ, USA). Both adjuvants consist in a suspension of particles in water. When needed, ionic strength of adjuvant suspensions was adjusted to 150 mM with sodium chloride (NaCl, Merck, Germany).

2.2. Methods

2.2.1. Sample preparation

Both AH powders and surfaces elaborated by immobilizing particles from AH suspensions on a solid substrate were analyzed. AH powders were obtained from adjuvant suspensions by freeze

drying. Suspensions were frozen in liquid nitrogen and subjected to the following temperature program: from −50 °C to −50 °C during 3 h; from −50 °C to −5 °C during 15 h; from −5 °C to −5 °C during 12 h and from −5 °C to 23 °C during 3 h. Freeze drying was performed at a pressure $\leq 6.10^{-3}$ mbar.

AH-based surfaces were prepared by coating gold-covered silicon wafers with adjuvant particles from suspensions. Gold-covered silicon wafers were produced in cleanroom facilities (WINFAB technological platform, Université catholique de Louvain). Silicon wafers were cleaned 2 times 10 min in a mixture of H_2SO_4/H_2O_2 followed by 30 s rinsing with HF 2% (v:v). Clean wafers were then covered by successive evaporation of a 10 nm layer of Ti and a 100 nm layer of Au (Dual E-gun evaporation system, VACOTEC, Rotselaar, Belgium). Gold-covered wafers were coated with a protective phenol-formaldehyde resin before being diced in 1 cm^2 square pieces, to avoid Si particles spreading on the gold surface. Before use, the resin was taken off by consecutive rinsings with acetone, methanol and ultrapure water. Gold substrates were then washed for 2 min with a mixture of H_2SO_4 95% and H_2O_2 30% (2:1) (Sigma-Aldrich), rinsed with ultrapure water and exposed during 15 min to UV/O_3 (UVO cleaner, Jelight Company, USA) just before coating. Gold was then coated by electrostatically-driven deposition of AH particles. 2 ml of AH suspension adjusted at pH 4 were added to a spectrophotometric cuvette to entirely cover the gold substrate, placed vertically in the cuvette. Adsorption was conducted during one hour. AH-coated wafers were then rinsed with ultrapure water and dried under a gentle nitrogen flow. In some cases, the ionic strength of the AH suspension was adjusted to 150 mM using NaCl.

2.2.2. Surface chemical composition determined by X-ray photoelectron spectroscopy (XPS)

Atomic composition of aluminum hydroxide samples was determined using a SSX 100/206 photoelectron spectrometer from Surface Science Instruments (USA) equipped with a monochromatized microfocused Al X-ray source (powered at 20 mA and 10 kV), a 30° solid angle acceptance lens, a hemispherical analyzer and a position-sensitive detector. The powder samples pressed in small stainless steel troughs of 4 mm diameter were placed on an insulating ceramic carousel (Macor® Switzerland). AH-coated gold substrates were stuck onto the ceramic carousel with double-sided adhesive tape. The pressure in the analysis chamber was around 10^{-6} Pa. The angle between the surface normal and the analyzer lens axis was 55°. The analyzed area was approximately 1.4 mm^2 and the pass energy was set at 150 eV (for survey spectra) or 50 eV (for individual spectra). A flood gun set at 8 eV and a Ni grid placed 3 mm above the sample surface were used for charge stabilization. In these conditions, the probed depth was around 10 nm.

The following sequence of spectra was recorded: survey spectrum, C 1s, O 1s, Al 2p and C 1 s again to check the charge compensation stability with time and the absence of sample degradation. Depending on the samples, Au 4f, S 2p, Na 1s, Cl 2p and F 1s peaks were also recorded. The C-(C,H) component of the C 1s peak of carbon was fixed to 284.8 eV to set the binding energy scale. Data treatment was performed with the CasaXPS program (Casa Software Ltd, UK), some spectra were decomposed with the least squares fitting routine provided by the software with a Gaussian/Lorentzian (85/15) product function and after subtraction of a Shirley baseline. Molar fractions were calculated using peak areas normalized on the basis of acquisition parameters and sensitivity factors provided by the manufacturer.

2.2.3. Morphology revealed by atomic force microscopy and scanning electron microscopy

Topographic images of AH samples were recorded using atomic force microscopy (AFM). AH-coated gold substrates were observed with a Nanoscope V multimode microscope (Digital Instruments, Santa Barbara, USA) in tapping mode using AFM probes with a spring constant of 10–130 N m^{-1} and resonant frequency in air from 204 to 497 kHz (Nanosensors, Neufchâtel, Switzerland). Images were treated with the Nanoscope analysis software and submitted to 3rd order flattening.

Scanning electron microscopy (SEM) images were recorded on a LEO 982 scanning electron microscope (Zeiss, Germany). Images were recorded on (i) AH powders obtained by freeze drying and deposited on a conductive double-sided adhesive tape, or (ii) AH suspensions spin-coated with a WS-400B-6NPP/Lite spin-coater (Laurell Technologies Corporation, North Wales, USA) during 1 min at 3000 rpm on glass coverslips previously cleaned as for gold substrates. A 6 nm-thick chromium layer was sputtered on both types of sample before analysis. The acceleration of the SEM electron beam was set at 2 kV.

2.2.4. Nitrogen adsorption and desorption analysis

The specific surface area of AH powders was determined using a nitrogen physisorption TriStar 3000 apparatus (Micromeritics, USA) operated at −196 °C. Freeze-dried adjuvant powders were degassed overnight at 150 °C under vacuum (50 mTorr). Adsorption and desorption of nitrogen molecules were recorded and plotted as adsorption isotherms. Specific surface area was determined by applying the Brunauer, Emmet and Teller (BET) model (between 0.05 and 0.30 p/p_0, where p is the nitrogen pressure at equilibrium and p_0 the saturation pressure) to these adsorption isotherms.

3. Results and discussion

3.1. Chemical composition of AH adjuvants determined by XPS

Surface chemical composition of AH adjuvant powders as well as of surfaces prepared by deposition of adjuvant suspensions on gold substrates was determined by XPS analysis and is shown in Table 1.

For AH powders, aluminum and oxygen are the major constituents detected. Oxygen can be divided into oxygen linked to aluminum (O—Al, from the adjuvant) and oxygen from environmental organic contamination (O—C). Oxygen from organic contamination was evaluated by decomposition of the carbon peak into oxygen-containing (C—O, C=O, O—C—O) and aliphatic (C—C,H) contributions. O—C oxygen amount was considered as equal to C—O + C=O + O—C—O contributions. Oxygen linked to aluminum (O—Al) was then obtained by subtracting the amount of O—C from the total amount of oxygen detected. Carbon, sodium, chlorine, sulfur, nitrogen and fluorine detected for AH powders are not constitutive of AH particles and are considered as contaminants coming from the adjuvant production process (Na, Cl, S, F) or manipulation of powders in the environment (C, N).

For surface-immobilized AH particles, oxygen and aluminum are still present in high amount. Gold from the substrate is also

Table 1
Elemental composition (molar fraction in %) of AH powders or gold substrates covered with AH suspensions determined by XPS analysis. Results are means for $n \geq 3$ (RSD Al and $O \leq 10\%$). bdl stands for "below detection limit".

Powders	Al	O—Al	O—C	C	Na	Cl	S	N	F
AH1	23.36	62.14	3.96	9.32	0.01	0.32	0.48	0.42	0.18
AH2	22.52	63.80	3.16	8.48	0.91	1.07	bdl	bdl	0.72
Particles on gold substrate			Al	O—Al	O—C	C	Au		
AH1	0 mM NaCl		16.70	46.84	3.90	23.40	9.05		
	150 mM NaCl		16.27	47.43	4.01	20.06	12.22		
AH2	0 mM NaCl		18.83	52.51	4.61	22.68	1.37		
	150 mM NaCl		16.27	50.84	3.29	23.06	6.53		

detected, which means that the surface coverage obtained after AH deposition on gold-covered substrates is not complete, or that the deposited layer is, at least locally, thinner than 10 nm. The only contaminant detected is carbon, other elements being left in the suspension used for deposition or washed away during the rinsing steps in the preparation of samples. The carbon content is higher for surface-deposited adjuvant particles than for adjuvant powders. Several studies have addressed the carbon contamination issue, which is affected by numerous factors. Among them, the nature of the surface, the surface charges of the analyzed area, the sample electrical conductivity and the developed surface area are known to play an important role (Callewaert et al., 2005; Denis et al., 2005; Landoulsi et al., 2016). For example, it is commonly observed that the more the sample is divided, i.e. the higher the developed surface area, the lower the carbon contamination level. In our case, powders probably develop more surface area than particles deposited on gold-covered substrates, and thus present a lower carbon contamination. The presence of exposed gold areas could also be responsible for the higher carbon contamination of AH-coated surfaces.

An important observation is the higher gold amount detected for substrates coated with suspensions at 150 mM NaCl, compared to suspensions deposited without NaCl. This leads to two hypotheses: first, the deposited layer thickness may decrease in presence of NaCl and, second, AH particles distribution over the gold-covered substrate is less homogeneous when NaCl was added to the suspensions, leaving more uncovered gold areas. Considering AH aggregate and particle sizes reported in the literature, as well as our own data from microscopy (see hereunder), the first hypothesis seems irrelevant. The second hypothesis of a less homogeneous distribution of particles could be explained by decreased AH particle adsorption on gold in presence of NaCl, or by AH particle aggregation in suspension promoted by NaCl, before deposition on gold surfaces. Compared to the adsorption of isolated particles, the adsorption of aggregates would statistically leave more uncovered gold areas. Indeed, randomly adsorbed aggregates partly cover the surface and once a given surface coverage is reached, they block the access to the interface to free aggregates. At that stage of the adsorption process, only smaller aggregates or isolated particles could still find enough space at the interface to adsorb. In absence of single isolated particles due to aggregation, the obtained adsorbed layer presents uncovered gold areas between aggregates.

In order to analyze more precisely the surface chemical composition of AH adjuvants, it is convenient to present the results as atomic ratios. Fig. 1 presents the Al to O-Al ratio (Al/O) obtained for powders and for surfaces prepared from adjuvant

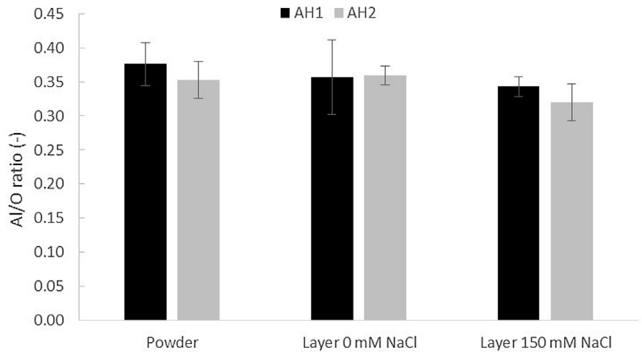

Fig. 1. Aluminum to oxygen ratio obtained after XPS analysis of AH adjuvants in powders or deposited on gold substrates. From left to right, Al/O ratio for powders of both AH, Al/O ratio for gold substrates coated with AH suspensions at 0 mM NaCl and Al/O ratio for gold substrates coated with AH suspensions at 150 mM NaCl. Error bars are standard deviation ($n \geq 3$).

suspensions. Pure $Al(OH)_3$ is expected to present an Al/O ratio of 0.33. All analyzed samples present an Al/O value around 0.35 regardless of NaCl presence. This value is close to the theoretical ratio expected for $Al(OH)_3$ and cannot be considered as significantly different. Ratios slightly higher than 0.33 may be obtained because of the presence, in AH adjuvants, of crystalline structures having an AlOOH formula. The apparition of the latter structure is due to hydrothermal treatment during the production process and is well described in the literature (Hem and White, 1995; Johnston et al., 2002; Shirodkar et al., 1990). Based on the work of Johnston et al. (Johnston et al., 2002), X-ray diffraction analysis was performed on AH powders and confirmed the presence of AlOOH structures (results not shown). A mixture of $Al(OH)_3$ and AlOOH leads to Al/O ratios between 0.33 and 0.5. Furthermore, the Al/O ratio is very similar for the different samples. This suggests that AH adjuvant chemistry (atomic composition and formula) is not modified or altered upon deposition on gold substrates. Changing the ionic strength of suspensions with NaCl before preparing surfaces has no effect on the resultant surface chemistry either.

3.2. Morphology of AH adjuvant particles

Fig. 2 presents scanning electron microscope (SEM) images obtained for both AH adjuvant powders and for AH suspensions at 0 mM NaCl spin-coated on a glass substrate. Freeze-dried particles of both AH show a fibrous morphology and are forming a 3D network. Spin-coated samples show less relief of particles due to the speed to which they were submitted to upon spin-coating, but adjuvant particles still present the same fibrous morphology and 3D organization. Primary needle-like particles are not observable on these images. The size of smaller aggregates is also quite difficult to measure, probably because of the chromium layer used to metallize the samples. The global shape observed by SEM for AH structures is consistent with previous morphological studies performed with transmission electron microscopy (Shirodkar et al., 1990) that highlighted the fibrous morphology of boehmite and pictured AH adjuvant as a network of needle-like particles forming fibrous aggregates in solution.

Fig. 3 shows atomic force microscopy images of samples prepared by deposition of AH particles on gold substrates. AFM was chosen as imaging technique, first because of its excellent resolution which may better reveal the surface morphology than SEM, and second to avoid the deposition of a chromium layer. As previously mentioned, in order to assess the effect of NaCl, i.e. of ionic strength, AH suspensions were deposited on gold substrates before (Fig. 3A and B) and after (Fig. 3C and D) addition of 150 mM NaCl.

The images show that AH1 particles are more aggregated after deposition from suspension than AH2 particles. Several 200 nm-high particle aggregates are observed on AH1-coated gold surfaces while AH2-coated surfaces are smoother. No significant aggregation is observed for AH2 particles. On inserts at higher magnification, it can be observed that AH adjuvants are composed of small globular and elongated particles of less than 50 nm. These globular particles may correspond to the previously mentioned “functional units” of adjuvants formed by the aggregation of needle-like primary particles (Morefield et al., 2004). Their size corresponds to observations made with transmission electron microscopy by Shirodkar et al. (Shirodkar et al., 1990). No significant difference is observed between these AH1 and AH2 particles.

The effect of NaCl on adjuvant suspension was investigated. 200 nm-high aggregates of globular particles are observed for AH1-coated substrate without NaCl (Fig. 3A). These aggregates are surrounded by single globular particles so that the gold surface seems almost fully covered with aluminum hydroxide. For AH1 at 150 mM NaCl (Fig. 3C), aggregates are bigger, i.e. higher than

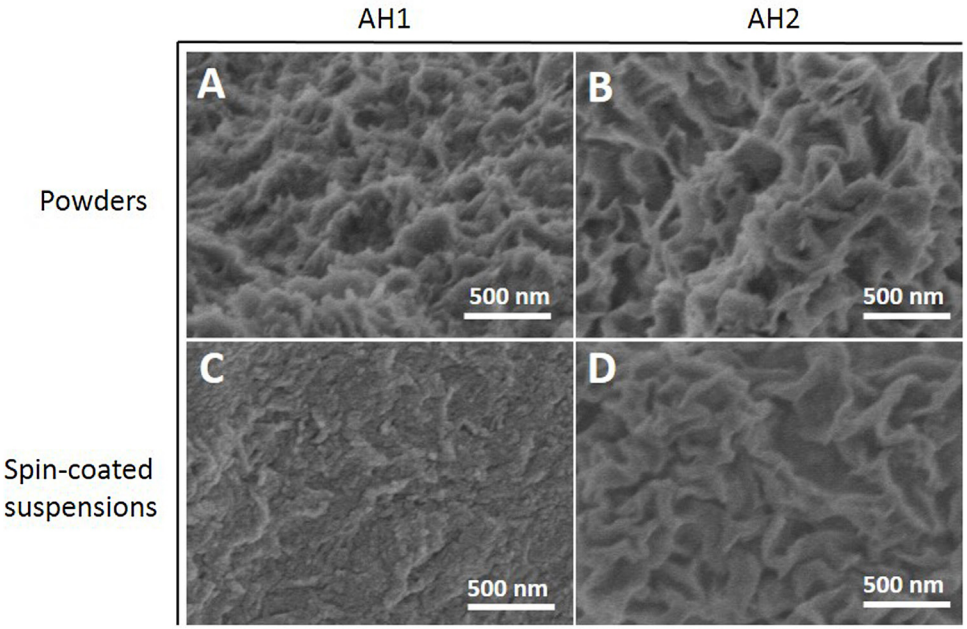

Fig. 2. SEM images of AH1 (A, C) and AH2 (B, D) adjuvants. A, B: powders obtained by freeze drying. C, D: suspensions spin-coated on glass substrate.

200 nm, and only a small number of single globular particles remains on the substrate, the space left between aggregates corresponding to the topography of the gold surface (see Supporting Info Figs. S1-S4). On images at higher magnification (Fig. 3 A and C–inserts), AH particle aggregation is clearly observed. This result is consistent with the observation of the higher gold content detected by XPS (from 9 to 12% of Au) on surfaces prepared with AH1 suspension at I adjusted to 150 mM compared to 0 mM

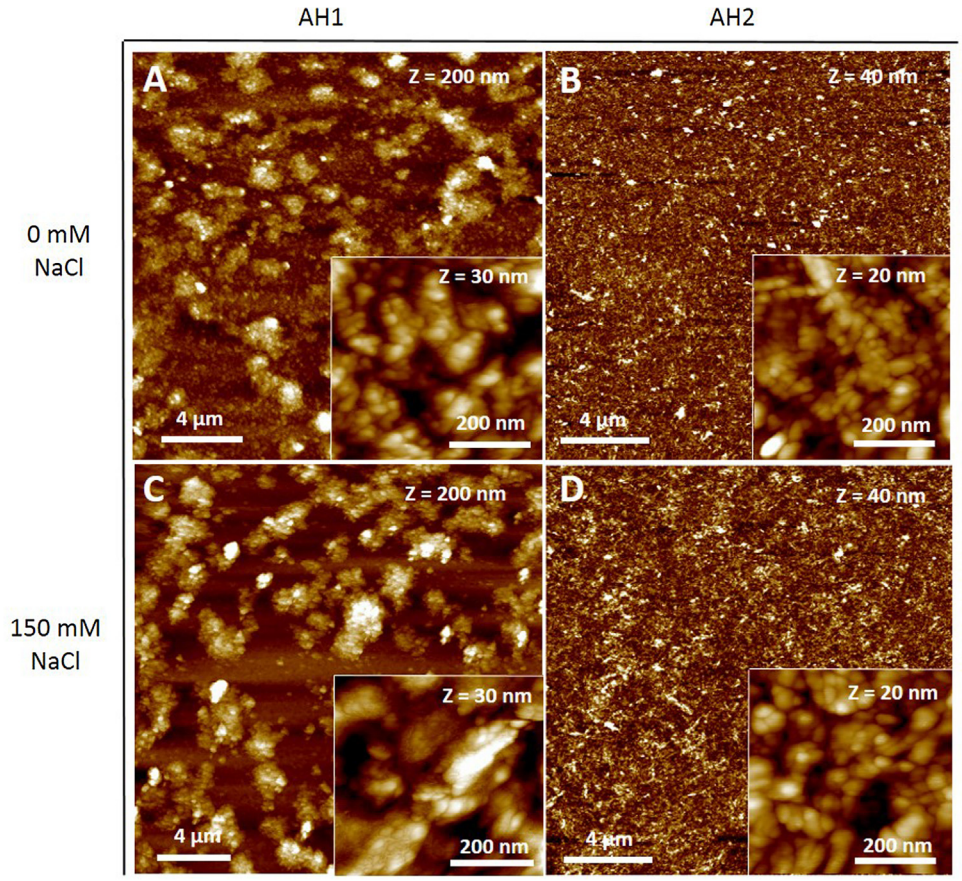

Fig. 3. AH1-coated (A, C) and AH2-coated (B, D) gold substrates imaged by AFM. Ionic strength of the adjuvant suspensions was kept to about 0 mM (A, B) or adjusted to 150 mM with NaCl (B, D) before deposition. Inserts in the lower right corner were recorded at higher magnification on the same sample.

(see Table 1). It is thus clear from XPS and AFM results that NaCl addition to the suspension leads to AH1 particle aggregation, and to the deposition of such aggregates with almost no smaller particles in between. The near absence of smaller particles could be due to their complete aggregation or to a potential role played by NaCl in preventing smaller particles to adsorb to the surface.

For AH2 adjuvant, particle aggregation in presence of NaCl is less clear on the AFM images. Higher magnification images do not present different aggregation state between both AH2 conditions. No aggregates are observed at all when NaCl is absent (Fig. 3B). However, cross sections performed on these images (Fig. 3B and D) show that the height of deposited structures observed on the sample prepared with 150 mM NaCl (Fig. 3D) is increased (see detailed analysis in Supporting Info, Fig. S5 and S6). Despite the less marked aggregation revealed by the morphological analysis of AH2 compared to AH1, XPS results obtained on these AH2 surfaces (Table 1) also show a higher gold content on samples prepared with 150 mM NaCl. This could be a consequence of AH particle aggregation in presence of NaCl, leaving more uncovered gold areas. A further evidence for particle aggregation in the case of AH2 can be observed in Fig. 4, showing a picture of two vials containing 5 ml of AH2 suspensions in absence or presence of 150 mM NaCl. When reversing the two vials, the suspension without I adjustment stays fluid and drops down, while the suspension at 150 mM ionic strength becomes highly viscous and does not flow anymore. A gel is obtained, demonstrating AH2 particle aggregation in presence of NaCl. The morphological similarity observed on AFM images of AH2 deposited from 0 mM or 150 mM NaCl (Fig. 3B and D) would be explained as follows: deposition on a gold substrate of the aggregated suspension was altered by the high viscosity of the suspension. The high viscosity leads to less mobility of AH2 aggregates towards the gold surface. Only the smaller particles present at the gel-surface interface can be deposited on the gold-covered substrate.

The morphological study combined with the chemical analysis of particles deposited on gold thus reveal that the presence of NaCl used to adjust the ionic strength of aluminum hydroxide adjuvant suspensions, as it is done in vaccine production process, promotes the aggregation of AH particles in suspension.

3.3. Specific surface area developed by AH samples

In the previous section, we demonstrated by both chemical and morphological analyses that NaCl promotes AH particles aggregation. This aggregation should be correlated with a decrease of the developed surface area of AH adjuvant in presence of 150 mM NaCl. Adsorption and desorption of nitrogen molecules was performed on powders obtained from suspensions at 0 and 150 mM NaCl to further determine their specific surface area by applying BET modeling. Fig. 5 presents the values of specific surface area obtained for the AH1 and AH2 powders at the two I values. The specific surface area of both AH adjuvants strongly decreases when I is adjusted to 150 mM with NaCl. Surface area drops from around 350 m^2/g to 225 m^2/g for AH1 particles, and is almost divided by two for AH2 adjuvant (from around 300 m^2/g at 0 mM down to 150 m^2/g at 150 mM NaCl).

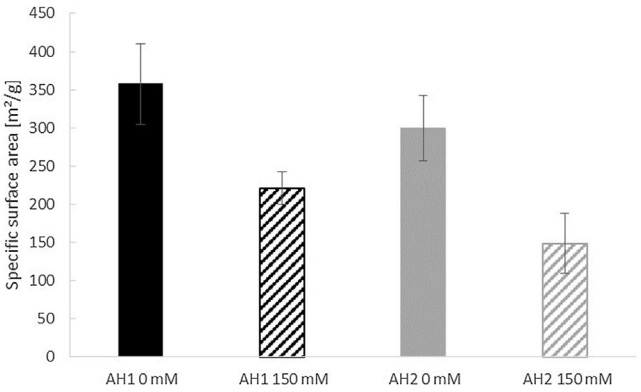

Fig. 5. Specific surface area [m^2/g] of AH1 and AH2 powders at 0 and 150 mM NaCl determined by application of BET model on nitrogen adsorption isotherms. Error bars are standard deviation (n = 3).

Previous works argued that specific surface area cannot be correctly measured by nitrogen adsorption method on aluminum-based adjuvants because of the impossibility to completely remove water molecules trapped in the adjuvant structure, and because of a strong adjuvant particle aggregation upon freeze-drying (Johnston et al., 2002). Freeze-drying of AH adjuvant without particle aggregation is possible in presence of trehalose as an excipient (Li et al., 2015). However, this addition of trehalose would unfortunately be an issue to determine AH specific area. The aim of our work was to see if the presence of NaCl had an effect on the developed surface area more than to precisely determine an absolute value for this specific area. Moreover, three adsorption isotherms with the same observed trend were obtained for each AH adjuvant. The decrease of specific surface area in presence of NaCl in adjuvant suspension is clearly demonstrated. It can be explained by adjuvant particle aggregation in suspension before freeze drying, and is consistent with AFM and XPS results presented in this work.

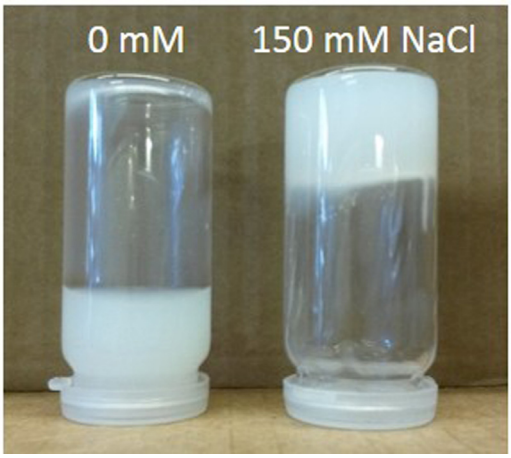

Fig. 4. AH2 suspension at 0 mM (left) and at 150 mM NaCl (right).

3.4. AH particle aggregation in presence of NaCl – mechanism and consequences

The present work shows that adding NaCl to AH adjuvant suspensions to adjust the ionic strength of vaccine promotes the aggregation of AH particles in suspension. The latter aggregation was directly observed on AFM images, was deduced from surface chemistry analysis of particles deposited on gold, and was correlated with an important decrease of the specific surface area developed by AH adjuvants. AH particle aggregation in presence of NaCl can be explained by the decrease of electrostatic repulsion between particles at higher I. Indeed, as Rinella et al. measured a PZC around 11.4 (Rinella et al., 1998), AH particles in suspension are positively charged in water and repel each other. Adding Na^+ and Cl^- ions leads to surface charge screening, reduces the Debye length and thus decreases the distance over which electrostatic

repulsion is effective. Aggregation can then occur, driven by van der Waals attraction forces.

Finally, AH aggregation seems really important even at moderate NaCl concentration (150 mM NaCl i.e. close to physiological I). This effect of NaCl on adjuvant structure was not studied before nor mentioned in previous works studying adsorption mechanisms of model proteins of aluminum-based adjuvants. The decrease of protein adsorption at physiological pH while rising I with NaCl was considered in the literature as a proof of the implication of electrostatic forces in the antigen adsorption process (Al-Shakhshir et al., 1995). The aggregation of AH particles and the consequent decrease of developed surface area would probably also lead to a reduced amount of adsorbed antigen in suspension. The modification of adjuvant structure needs therefore to be taken into account for the determination of antigen adsorption mechanisms on aluminum-based adjuvants. AH aggregation effect in presence of NaCl is also important in industrial vaccine formulation. AH structure alteration when adjusting I after antigen adsorption may lead to antigen desorption and to a decrease of vaccine efficiency. Free antigen amount should be evaluated in formulated vaccine after I adjustment.

4. Conclusion

In conclusion, morphological and surface chemical characteristics of two different AH adjuvants were determined in this work. Both adjuvant powders present similar shape of particles, surface chemical composition and Al/O ratios. The effect of 150 mM NaCl on the physicochemical properties of these adjuvants was investigated. Taken together, the results show that NaCl treatment leads to AH adjuvant particle aggregation. This is indeed demonstrated by (i) the sol-gel transition of AH2 suspension observed upon NaCl addition, (ii) the lower surface coverage of gold after deposition of NaCl-treated AH particles revealed by XPS and AFM, and (iii) the decrease of the surface specific area of AH powders after NaCl treatment.

Aggregation of AH adjuvants is thus triggered in presence of NaCl at a concentration close to body isotonicity. This effect on the adjuvant structure should be taken into account when studying the adsorption mechanisms of protein antigens on aluminum-based adjuvants and during vaccine formulation processes. In the literature, the decrease of model protein adsorption on adjuvant particles at physiological pH in presence of NaCl was only attributed to the main role played by electrostatic forces in the adsorption process. The effect of NaCl on the adjuvants demonstrated in this work needs however to be considered. The effect of ionic strength adjustment on antigen adsorption, which depends on adjuvant characteristics, should also be addressed in vaccine formulation.

This work also opens perspectives for further advanced surface characterization of AH adjuvant particles and for the study of antigen adsorption on adjuvant particles. The deposition of AH particles on gold substrates by electrostatically-driven deposition is indeed promising to elaborate homogeneous thin layers of adjuvant particles with preserved chemistry, with the intent to use advanced surface analysis techniques.

Acknowledgements

The authors thank the BRENNTAG company for kindly providing the ALHYDROGEL® "85" material. Many thanks to the Molecule, Solids and Reactivity (MOST) division of the Institute of Condensed Matter and Nanosciences (IMCN), and particularly to Pr. Eric Gaigneaux, Josefine Schnee, François Devred and Benjamin Farin, from Heterogeneous Catalysis Research Group, for the help with the TriStar apparatus and nitrogen adsorption isotherms analysis. The work was supported by the Belgian Science Policy through the Interuniversity Attraction Pole Program (P07/05) and by the Belgian National Foundation for Scientific Research (FNRS).

Appendix A. Supplementary data

Supplementary data associated with this article can be found, in the online version, at http://dx.doi.org/10.1016/j.ijpharm.2016.12.019.

Bibliography:

Aguilar, J.C., Rodríguez, E.G., 2007. Vaccine adjuvants revisited. Vaccine 25, 3752–3762.
Al-Shakhshir, R.H., Regnier, F.E., White, J.L., Hem, S.L., 1995. Contribution of electrostatic and hydrophobic interactions to the adsorption of proteins by aluminium-containing adjuvants. Vaccine 13, 41–44.
Burrell, L.S., Lindblad, E.B., White, J.L., Hem, S.L., 1999. Stability of aluminium-containing adjuvants to autoclaving. Vaccine 17, 2599–2603.
Burrell, L.S., Johnston, C.T., Schulze, D., Klein, J., White, J.L., Hem, S.L., 2000a. Aluminium phosphate adjuvants prepared by precipitation at constant pH. Part I: composition and structure. Vaccine 19, 275–281.
Burrell, L.S., Johnston, C.T., Schulze, D., Klein, J., White, J.L., Hem, S.L., 2000b. Aluminium phosphate adjuvants prepared by precipitation at constant pH. Part II. physicochemical properties. Vaccine 19, 282–287.
Burrell, L.S., White, J.L., Hem, S.L., 2000c. Stability of aluminium-containing adjuvants during aging at room temperature. Vaccine 18, 2188–2192.
Callewaert, M., Gerin, P.A., Genet, M.G., Boulangé-Petermann, L., Rouxhet, P.G., 2005. Première Conf. sur les Spectroscopies de Photoélectrons. ELSPEC, Paris (2004, SFV Editions).
Clausi, A., Cummiskey, J., Merkley, S., Carpenter, J.F., Braun, L.J., Randolph, T.W., 2008. Influence of particle size and antigen binding on effectiveness of aluminum salt adjuvants in a model lysozyme vaccine. J. Pharm. Sci. 97, 5252–5262.
Denis, F.A., Genet, M.G., Rouxhet, P.G., 2005. Première Conf. Francophone sur les Spectroscopies de Photoélectrons. ELSPEC, Paris, pp. 173–177 (2004, SFV Editions).
Eppstein, D.A., Byars, N.E., Allison, A.C., 1989. Use of peptides and proteins as drugs, part I new adjuvants for vaccines containing purified protein antigens. Adv. Drug Deliv. Rev. 4, 233–253.
Hem, S.L., HogenEsch, H., 2007. Relationship between physical and chemical properties of aluminum-containing adjuvants and immunopotentiation. Expert Rev. Vaccines 6, 685–698.
Hem, S.L., White, J.L., 1995. Stucture and properties of aluminum-containing adjuvants. In: Powell, M.F., Newman, M.J. (Eds.), Vaccine Design: The Subunit and Adjuvant Approach. Plenum Press, New York, pp. 249–276.
HogenEsch, H., 2002. Mechanisms of stimulation of the immune response by aluminum adjuvants. Vaccine 20, S34–S39.
Iyer, S., HogenEsch, H., Hem, S.L., 2003. Effect of the degree of phosphate substitution in aluminum hydroxide adjuvant on the adsorption of phosphorylated proteins. Pharm. Dev. Technol. 8, 81–86.
Johnston, C.T., Wang, S.-L., Hem, S.L., 2002. Measuring the surface area of aluminum hydroxide adjuvant. J. Pharm. Sci. 91, 1702–1706.
Jones, L.S., Peek, L.J., Power, J., Markham, A., Yazzie, B., Middaugh, C.R., 2005. Effects of adsorption to aluminum salt adjuvants on the structure and stability of model protein antigens. J. Biol. Chem. 280, 13406–13414.
Landoulsi, J., Genet, M.J., Fleith, S., Touré, Y., Liascukiene, I., Méthivier, C., Rouxhet, P. G., 2016. Organic adlayer on inorganic materials: XPS analysis selectivity to cope with adventitious contamination. Appl. Surf. Sci. 383, 71–83.
Li, X., Thakkar, S.G., Ruwona, T.B., Williams Iii, R.O., Cui, Z., 2015. A method of lyophilizing vaccines containing aluminum salts into a dry powder without causing particle aggregation or decreasing the immunogenicity following reconstitution. J. Controlled Release 204, 38–50.
Lindblad, E.B., 2004. Aluminium adjuvants–in retrospect and prospect. Vaccine 22, 3658–3668.
Mbow, M.L., De Gregorio, E., Valiante, N.M., Rappuoli, R., 2010. New adjuvants for human vaccines. Curr. Opin. Immunol. 22, 411–416.
Morefield, G.L., HogenEsch, H., Robinson, J.P., Hem, S.L., 2004. Distribution of adsorbed antigen in mono-valent and combination vaccines. Vaccine 22, 1973–1984.
Morefield, G.L., Jiang, D., Romero-Mendez, I.Z., Geahlen, R.L., HogenEsch, H., Hem, S. L., 2005. Effect of phosphorylation of ovalbumin on adsorption by aluminum-containing adjuvants and elution upon exposure to interstitial fluid. Vaccine 23, 1502–1506.
O'Hagan, D.T., MacKichan, M.L., Singh, M., 2001. Recent developments in adjuvants for vaccines against infectious diseases. Biomol. Eng. 18, 69–85.
Rinella Jr, J.V., White, J.L., Hem, S.L., 1998. Effect of pH on the elution of model antigens from aluminum-containing adjuvants. J. Colloid Interface Sci. 205, 161–165.
Shirodkar, S., Hutchinson, R.L., Perry, D.L., White, J.L., Hem, S.L., 1990. Aluminum compounds used as adjuvants in vaccines. Pharm. Res. 7, 1282–1288.
Singh, M., Ugozzoli, M., Kazzaz, J., Chesko, J., Soenawan, E., Mannucci, D., Titta, F., Contorni, M., Volpini, G., Guidice, G.D., O'Hagan, D.T., 2006. A preliminary

evaluation of alternative adjuvants to alum using a range of established and new generation vaccine antigens. Vaccine 24, 1680–1686.
Sivakumar, S.M., Safhi, M.M., Kannadasan, M., Sukumaran, N., 2011. Vaccine adjuvants–current status and prospects on controlled release adjuvancity. Saudi Pharm. J. 19, 197–206.
Tettenhorst, R., Hofmann, D.A., 1980. Crystal chemistry of boehmite. Clays Clay Miner. 28, 373–380.
Yau, K.P., Schulze, D.G., Johnston, C.T., Hem, S.L., 2006. Aluminum hydroxide adjuvant produced under constant reactant concentration. J. Pharm. Sci. 95, 1822–1833.